VI International Conference on Computational Methods for Coupled Problems in Science and Engineering
COUPLED PROBLEMS 2015
B. Schrefler, E. Oñate and M. Papadrakakis (Eds)

ON THE PSEUDO-INCIDENT WAVE TECHNIQUE FOR INTERACTING INHOMOGENEITIES IN ELECTROMECHANICAL PROBLEMS

XIAODONG WANG*, HUANGCHAO YU, S. ABDEL-GAWAD AND CHEN WANG

Department of Mechanical Engineering, University of Alberta
Edmonton, Alberta, Canada T6G 2G8
*e-mail: xiaodong.wang@ualberta.ca

Key words: Interaction, Elastic Wave, Electromechanical Problems, Inhomogeneities, Numerical Methods.

Abstract. The current paper presents the Pseudo-Incident Wave method for the theoretical treatment of the dynamic interaction between general inhomogeneities in advanced piezoelectric structures. Instead of simulating the response of such complicated systems using purely numerical or analytical methods, the current technique will take the advantages of the accuracy and reliability of analytical solutions and the flexibility of numerical methods. Using this method the original interaction problem is reduced to the solution of coupled single inhomogeneity problems, for which analytical solutions or simpler numerical solutions could be derived. By considering the consistency condition between different inhomogeneities, the steady state dynamic solution of multiple interaction problems can be formulated in terms of coupled single inhomogeneity solutions. The current method is very general and can provide reliable simulation of complicated interaction problems. Numerical examples are presented to illustrate the effectiveness of the Pseudo-Incident Wave method in simulating dynamic interaction between general inhomegeneities under complicated geometries.

1 INTRODUCTION

Piezoelectric materials are widely used in advanced structures to form self-monitoring and self-controlling smart systems and have drawn considerable attention from the research community. Mechanical deformation of such materials can be directly converted into electric signals for monitoring the mechanical deformation. In the reverse process, an applied electric field could induce deformation in the material. Therefore, the designers of such advanced structures will constantly face the challenge of properly modeling the electromechanical coupling between the electric and mechanical fields.

One of the most fundamental issues surrounding the optimization of the effectiveness and reliability of piezoelectric structures with multiple piezoelectric components is the evaluation of the effect of the interaction between different inhomogeneities, which will significantly affect both the local and global response of the coupled system. An accurate assessment of the coupled electromechanical behavior of an integrated piezoelectric composite system would, therefore, require the determination of the local stress and electric fields involving interacting inhomogeneities.

Significant efforts had been made to the study of the quasistatic electromechanical behavior of piezoelectric composite materials. For example, the problems of a single elliptical (ellipsoidal) inhomogeneity in unbounded piezoelectric materials were solved using the Green's function approach [1, 2], the effective properties of piezoelectric composites was determined using different micromechanical models [3-6], and the fracture and damage of piezoelectric materials was also studied [7]. However, relatively few studies have focused on the interaction between inhomogeneities, especially the dynamic interacting behavior of inhomogeneities. It should be noted, however, that piezoelectric structures are currently being used or intended to use in situations where dynamic loading is involved, such as smart structures under impact loading and the acoustic control of smart skin systems. Even for static cases, it was observed that for composite material systems the mechanical properties are more sensitive to the local response of individual inhomogeneities [8, 9], which is closely related to the interaction among inhomogeneities.

The mechanical and electrical properties of advanced piezoelectric composite structures are greatly affected by the attached piezoelectric sensors/actuators, debondings, fibres and/or embedded cracks. The interaction between these inhomogeneities will cause the redistribution of the local stress and electric fields, which results in mechanical shielding or amplification effects and affects the overall failure mechanism, and alters the electrical behavior of the structures. Because of the complexity of the problem, when dynamic loads are applied, the simulation of the dynamic response of such coupled systems possesses a significant challenge. Typical numerical methods, such as finite element method or boundary element method, can be used to conduct dynamic simulation of these problems under certain conditions but have their own limitations when multiple interactions are involved, because of the computing resource needed to obtain reliable results. Analytical study of interacting inhomogeneities under dynamic loads is very attractive because of its high reliability and accuracy, but is limited to only simple cases of single inhomogeneity of certain types.

It is therefore the objective of the present paper to provide a comprehensive treatment of the steady-state dynamic behavior of interacting inhomogeneities in piezoelectric composites. The original problem is decomposed into single inhomogeneity subproblems. The solutions of these subproblems are then implemented into a pseudo-incident wave method to account for the interaction between different inhomogeneities. Numerical examples are provided to show the effect of the interaction between inhomogeneities, the material mismatch and the loading frequency upon the dynamical field.

2 PROBLEM FORMULATION

Consider an infinitely extended piezoelectric medium containing $\overline{M}$ arbitrarily located circular piezoelectric inhomogeneities of radius R_m ($m=1,2, \dots, \overline{M}$), as shown in Fig.1. Inhomogeneity m and the matrix are bonded through a thin layer of thickness h_m. A global Cartesian (x, y) and local polar (r_m, θ_m) coordinate systems are used to characterize the inhomogeneities. The position of the center of inhomogeneity m is denoted (x_m, y_m) in the global coordinate system. The piezoelectric materials are assumed to be transversely isotropic with the axis of symmetry being perpendicular to the $x-y$ plane. The shear moduli, the piezoelectric constants, the dielectric constants and the mass densities of the matrix and the inhomogeneities are denoted as $c_{44}^M, e_{15}^M, \kappa_{11}^M, \rho^M$ and $c_{44}^F, e_{15}^F, \kappa_{11}^F, \rho^F$, respectively. The corresponding material constants of the interphase of inhomogeneity m are c_{44}^m, e_{15}^m and κ_{11}^m.

When subjected to a steady state load of frequency ω, the resulting fields will generally involve an exponential harmonic factor $\exp(-i\omega t)$. For the sake of convenience, this factor will be suppressed and only the amplitude of different field variables will be considered.

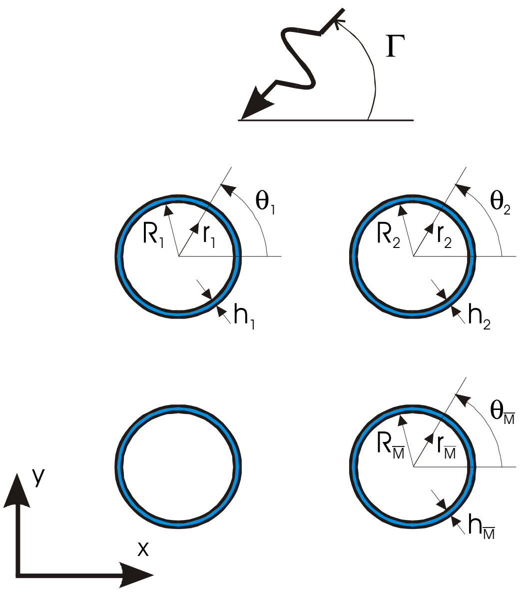

Figure 1: Interacting Piezoelectric Inhomogeneities

The steady state behavior of a homogeneous piezoelectric material under antiplane mechanical and inplane electric loading is fully described by the following governing equations:

$$\nabla^2 w + k^2 w = 0, \qquad \nabla^2 f = 0 \tag{1}$$

where the Laplacian operator ∇^2 stands for $\partial^2/\partial r^2 + \frac{1}{r}\partial/\partial r + \frac{1}{r^2}\partial^2/\partial\theta^2$, w is the antiplane displacement and k is the wave number defined by

$$k^2 = \frac{\rho\omega^2}{c_*} \quad \text{with} \quad c_* = c_{44} + \frac{e_{15}^2}{\kappa_{11}} \tag{2}$$

The electric potential ϕ is given by

$$\phi = \frac{e_{15}}{\kappa_{11}} w + f \tag{3}$$

and the corresponding non-vanishing stress and electric displacement components can be expressed as:

$$\tau_{rz} = c_* \frac{\partial w}{\partial r} + e_{15} \frac{\partial f}{\partial r} \quad \tau_{\theta z} = c_* \frac{1}{r} \frac{\partial w}{\partial \theta} + e_{15} \frac{1}{r} \frac{\partial f}{\partial \theta} \tag{4}$$

$$D_r = -\kappa_{11} \frac{\partial f}{\partial r}, \quad D_\theta = -\kappa_{11} \frac{1}{r} \frac{\partial f}{\partial \theta} \tag{5}$$

In these equations, $c_{44}, e_{15}, \kappa_{11}$ and ρ are the elastic modulus, the piezoelectric constants, the dielectric constant and the mass density, which should be replaced by the corresponding material constants of the matrix, the inhomogeneities and the interphases, respectively, when these media are considered.

3 INTERFACE MODEL

Interphases between matrix and fibers play a dominant role in characterizing the behavior of composites [10, 11]. In the current study, it is assumed that the thickness of interfacial layers is much smaller than the radius of fibers and the wavelength and that the inertial effect of the interfacial layers can be ignored. Accordingly, the radial shear stress τ_{rz}, strain γ_{rz}, electric displacement D_r and electric field intensity E_r are assumed to be uniform across the thickness of interphases, and the constitutive relation of interphase *m* can be expressed as

$$\begin{aligned} \tau_{rz}(\theta_m) = & \frac{c_*^m}{h_m} [w(R_m + h_m, \theta_m)|_{matrix} - w(R_m, \theta_m)|_{in\,\mathrm{hom}\,ogeneity}] \\ & + \frac{e_{15}^m}{h_m} [f(R_m + h_m, \theta_m)|_{matrix} - f(R_m, \theta_m)|_{in\,\mathrm{hom}\,ogeneity}] \end{aligned} \tag{6}$$

$$D_r(\theta_m) = -\frac{\kappa_{11}^m}{h_m} [f(R_m + h_m, \theta_m)|_{matrix} - f(R_m, \theta_m)|_{in\,\mathrm{hom}\,ogeneity}] \tag{7}$$

4 SINGLE INHOMOGENEITY PROBLEM

For a single inhomogeneity m subjected to an incident wave. The general solution of the displacement and electric fields can be expressed in terms of Fourier expansions in a local polar coordinate system (r_m, θ_m), as

$$w^m(r_m, \theta_m) = \begin{cases} \sum_{n=0}^{\infty} H_n^{(1)}(k_M r_m)[a_n^m e^{in\theta_m} + b_n^m e^{-in\theta_m}] + w^{inc} & \textit{in the matrix} \\ \sum_{n=0}^{\infty} J_n(k_F r_m)[c_n^m e^{in\theta_m} + d_n^m e^{-in\theta_m}] & \textit{in the in}\,\mathrm{hom}\,\textit{ogeneity} \end{cases} \tag{8}$$

$$f^m(r_m,\theta_m) = \begin{cases} \sum_{n=0}^{\infty} r_m^{-n}[f_n^m e^{in\theta_m} + g_n^m e^{-in\theta_m}] + f^{inc} & \text{in the matrix} \\ \sum_{n=0}^{\infty} r_m^{n}[p_n^m e^{in\theta_m} + q_n^m e^{-in\theta_m}] & \text{in the inhomogeneity} \end{cases} \tag{9}$$

where $H_n^{(1)}$ and J_n are Hankel function and Bessel function of the first kind, respectively. w^{inc} and f^{inc} represent the incident wave. The solution of $a_n^m, b_n^m, c_n^m, d_n^m$ and f_n^m, g_n^m, p_n^m and q_n^m can be obtained by making use of the interphase model, eqns. (6) and (7).

Truncating the Fourier expansion in (8) and (9) into *Nth* term, the solution of the governing parameters $a_n^m, b_n^m, c_n^m, d_n^m$ and f_n^m, g_n^m, p_n^m and q_n^m can then be expressed in terms of the incident wave at the following integral points

$$\theta_m^l = \frac{2\pi(l-1)}{L-1}, \quad l = 1,2,\ldots,L \tag{10}$$

as

$$\{C\}^m = [A]^m \{F\}^m \tag{11}$$

where $[A]^m$ is a known matrix, $\{C\}^m$ represents the coefficients of Fourier expansion of inhomogeneity m, given by

$$\{C\}^m = \{a_0^m, f_0^m, c_0^m, q_0^m, a_1^m, b_1^m, f_1^m, g_1^m, c_1^m, d_1^m, p_1^m, q_1^m, \ldots, c_N^m, d_N^m, p_N^m, q_N^m\}^T \tag{12}$$

and $\{F\}$ represents the general loads acting on the integral points given by (10), i.e.

$$\{F\}^m = \{\tau_1, D_1, \frac{\kappa_{11}^m}{h^m} w_1, f_1, \ldots, \tau_L, D_L, \frac{\kappa_{11}^m}{h^m} w_L, f_L\}^T \tag{13}$$

5 INTERACTING INHOMOGENEITIES

For the cases where multiple inhomogeneities are involved, the interaction between these inhomogeneities may significantly affect the electromechanical behavior of the composites.

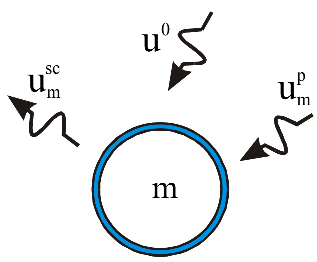

Figure 2: Pesudo-incident wave

5.1 Pseudo-incident wave method

Let us now focus our attention on a specific inhomogeneity m. The total incident wave for inhomogeneity m can be expressed as

$$u_m^I = u^0 + u_m^p \tag{14}$$

where u^0 is the initial incident wave and u_m^p is the unknown pseudo-incident wave from other inhomogeneities with u representing both the mechanical and the electric fields. As a result of this incident wave, inhomogeneity m will result in a scattering wave u_m^{sc}, as shown in Fig.2. The total field in the matrix can then be expressed as

$$u^{total} = u_m^I + u_m^{sc} = u^0 + u_m^p + u_m^{sc} \tag{15}$$

can also be obtained by summing up the initial field and the contributions from all inhomogeneities, such that

$$u^{total} = u^0 + \sum_{j=1}^{\overline{M}} u_j^{sc} \tag{16}$$

The equivalence between eqns. (15) and (16) indicates that

$$u_m^p = \sum_{j \neq m}^{\overline{M}} u_j^{sc}, \quad j = 1,2,...,\overline{M} \tag{17}$$

Equation (17) represents the relation between different inhomogeneities.

5.2 Solution of interacting inhomogeneities problems

According to eqns. (14) and (17), the general load $\{F\}^m$ used in eqn. (11) can be expressed as

$$\{F\}^m = \{F^0\}^m + \sum_{j \neq m}^{\overline{M}} \{F^{sc}\}_j^m \tag{18}$$

where $\{F^0\}^m$ is due to the original incident wave and $\{F^{sc}\}_j^m$ is the general load due to the scattered wave of inhomogeneity j. $\{F^{sc}\}_j^m$ can be obtained by using the general solution given by (8) and (9), and the constitutive relation (4) and (5) as

$$\{F^{sc}\}_j^m = [T]_j^m \{C\}^j \tag{19}$$

where $\{C\}^j$ represents the Fourier expansion coefficients of inhomogeneity j and $[T]_j^m$ is a known matrix obtained by rearranging (8) and (9). Substituting eqns. (18) and (19) into (11) results in

$$\{C\}^m - \sum_{j \neq m}^{\overline{M}} [A]^m [T]_j^m \{C\}^j = [A]^m \{F^0\}^m, \quad m = 1,2,...,\overline{M} \tag{20}$$

from which $\{C\}^m (m = 1,2,...,\overline{M})$ can be determined by solving a system of linear algebraic equations.

According to eqn. (16), the resulting mechanical and electric fields in the matrix given by eqns. (8) and (9) can be expressed in terms of the coefficients of Fourier expansions as

$$w(x,y)=w^{0}(x,y)+\sum_{m=1}^{\bar{M}}\sum_{n=0}^{N}H_{n}^{(1)}(k_{M}\bar{r}_{m})[a_{n}^{m}e^{in\bar{\theta}_{m}}+b_{n}^{m}e^{-in\bar{\theta}_{m}}] \tag{21}$$

and

$$f(x,y)=f^{0}(x,y)+\sum_{m=1}^{\bar{M}}\sum_{n=0}^{N}\bar{r}_{m}^{-n}[f_{n}^{m}e^{in\bar{\theta}_{m}}+g_{n}^{m}e^{-in\bar{\theta}_{m}}] \tag{22}$$

where

$$\bar{r}_{m}=\sqrt{(x-x_{m})^{2}+(y-y_{m})^{2}},\ \bar{\theta}_{m}=\operatorname{sgn}(y-y_{m})\cos^{-1}\frac{x-x_{m}}{\bar{r}_{m}} \tag{23}$$

From Eqns. (21) and (22), the stress and the electric displacement in the matrix can be obtained using the constitutive relation given by (4) and (5).

6 RESULTS AND DISCUSSIONS

The theoretical analysis described in previous section is used to investigate the coupled electromechanical response of piezoelectric composites to an incident harmonic wave, as shown in Fig. 1. The incident antiplane displacement and the electric potential can be expressed as

$$w^{(in)}=\frac{i\tau}{c_{*}^{M}k_{M}}e^{-ik_{M}(xcon\Gamma+y\sin\Gamma)},\ \phi^{(in)}=\frac{e_{15}^{M}}{\kappa_{11}^{M}}w^{(in)}$$

where τ is the maximum value of the shear stress carried by the incident wave, and Γ is the incident angle. In the following examples, uniformly distributed identical piezoelectric fibers will be examined. The present formulations predict the dependence of the electric and mechanical fields upon the geometry of the fibers, the material combination, the interfacial property, the frequency and angle of the incident wave. It should be recognized that only the amplitudes of the complex shear stress and electric potential are considered in the following figures.

6.1 Local Shear Stress

It is well known that local stress field in composites will be disturbed by the existence of fibers due to material mismatch [12]. The current study indicates that even when there no elastic mismatch exists, the electromechanical coupling between electric and mechanical fields in piezoelectric inhomoheneities may also result in significant change in the local stress level. Figure 3 shows the distribution of the scattering shear stress ($\tau^{*}=\tau_{rz}/\tau$) along the circumference of a single fiber embedded in an insulating medium subjected to an incident wave with $\Gamma=90^{0}$. The shear wave speeds (and shear moduli) of the fiber and the matrix are assumed to be same. In this figure, the normalized piezoelectric constant $\lambda=\{e_{15}^{F}\}^{2}/c_{*}^{F}\kappa_{11}^{F}$ is taken to be $\lambda=1$ and $k^{*}=Rk_{F}$ represents the normalized frequency of the incident wave. Unlike non-piezoelectric materials for which no scattering will be generated for the current material combination, the piezoelectric fiber results in shear stresses over 0.25τ at $\theta=30^{0}$ and 150^{0}. Significant stress distribution is also observed in Fig. 4, which shows the corresponding interfacial shear stress distribution along the surface of inhomogeneity one with the presence of inhomogeneity two. The distance between them is $0.2R$ with R being the radius of the inhomogeneities.

6.2 Electric field

Electric potential induced in a piezoelectric composite could be used to monitor the deformation of the material and the property of the incident wave. Figure 5 shows the distribution of the electric potential ($\phi^* = e_{15}^F \phi / R\tau$) along the boundary of a single fiber examined in Fig. 3. It is very interesting to note that the peak value of ϕ^* has a unique relation with the incident angle ($\Gamma = 90^0$) for different loading frequencies. Figure 6 shows the corresponding results for two interacting inhomogeneities, similar to the case discussed in Fig. 4. In this case, the relation between the incident angle and the position of the peak value of ϕ^* shows a strong frequency-dependence.

6.3 Multiple interaction of inhomogeneities

Interaction between multiple inhomogeneities was studied using the current method for mechanical problems. Figure 7 shows the displacement field (real part) of two interacting inhomogeneities with $Rk^M = 7.5, \Gamma = 90^0$ and the distance between the inhomogeneities being *R*. The distribution of displacement (amplitude) around the boundary of the left inhomogeneity for different distances between the inhomogeneities is given in figure 8. The asymmetry of the results indicates the effect of the interaction between the inhomogeneities. Figure 9 shows the displacement field caused by four interacting inhomogeneities with $Rk^M = 1.0, \Gamma = 90^0$, the distance between adjacent inhomogeneities being *0.5R* and the ratio of the wave speed (matrx/inhomogeneity) being *0.707*.

Interaction between multiple inhomogeneities, as shown in figure 10, is also considered, where the distance between the adjacent inhomogeneities is *R*. Figures 11 and 12 show the displacement field generated by the multiple interaction for $Rk^M = 0.59, \Gamma = 90^0$ and $Rk^M = 1.37, \Gamma = 90^0$, respectively. The incident wave is blocked by the inhomogeneity array for both frequencies, which are in the bandgap of the inhomogeneity array. The successful treatment of the interaction between large numbers of inhomogeneities clearly shows the advantage of the current method.

ACKNOWLEDGEMENT

This research was supported by the Natural Sciences and Engineering Research Council of Canada (NSERC) .

REFERENCES

[1] Deeg, W. F. *The Analysis of dislocation, crack and inclusion problems in piezoelectric solids*, Ph. D. Dissertation, Stanford University. (1980).

[2] Benveniste, Y. The determination of the elastic and electric fields in a piezoelectric inhomogeneity. *J. Appl. Phys*. (1992) **72**: 1086-1095.

[3] Dunn, M. and Taya, M. Micromechanical predictions of the effective electro elastic moduli of piezoelectric composites. *Int. J. Solid Struct*. (1993) **30**: 161-175.
[4] Pak, Y. E. Crack extension force in a piezoelectric media with defects. *Int. J. Solids Struct*. (1990) **28**: 491-505.
[5] Suo, Z., Kuo, C. M., Barnett, D. M. and Wills, J. R. Fracture mechanics for piezoelectric ceramics. *J. Mech. Phys. Solids*. (1992) **40**: 739-765.
[6] Jain, A. K. and Sirkis, J. S. Continuum damage mechanics in piezoelectric ceramics. *Adaptive Structures and Composite Materials: Analysis and Application*. ASME (1994) AD **45**/MD **54**: 47-58.
[7] He, M. Y., Suo, Z., McMeeking, R. M., Evans, A. G. and Lynch, C.S. The mechanics of some degradation mechanisms in ferroelectric ceramic actuators, *SPIE*, (1994) **2189**: 344-356.
[8] Kachanov, M., Sevostianov, I. Non-interaction approximation in the problem of effective properties. In: Kachanov, M., Sevostianov, I. (Eds.), *Effective Properties of Heterogeneous Materials.* Springer, Dordrecht. (2014) 1–96.
[9] Rodin G. J. and Weng, G. J. On reflected interactions in elastic solids containing inhomogeneities. *Journal of the Mechanics and Physics of Solids* (2014) **68**: 197–209.
[10] Matikas, T. E. Ultrasonic reflectively technique for the characterization of fiber-matrix interface in metal matrix composites. *J. Appl. Phys*. (1993) **74**: 228-236.
[11] Veazie, D. R. and Qu, J. Effects of interphase on the transverse stress-strain behavior in unidirectional fiber reinforced metal matrix composites. *Composites Engineering*. (1995) **5**: 597-610.
[12] Wang, X. D. and Meguid, S. A. Diffraction of SH-wave by interacting matrix crack and an inhomogeneity. *ASME J. Appl. Mech*. (1997) **64**: 568-575.

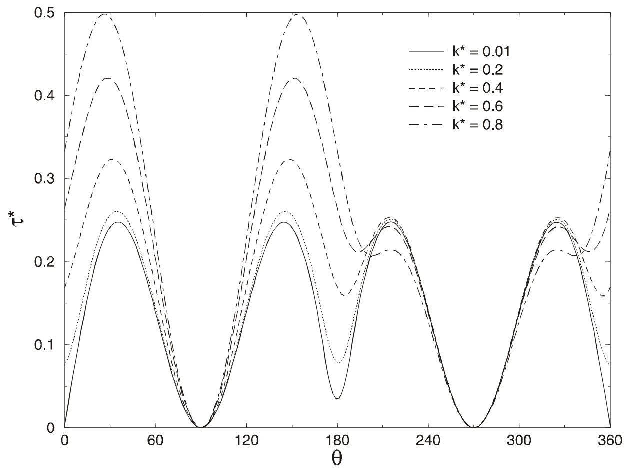

Figure 3: Shear stress of a single inhomogeneity

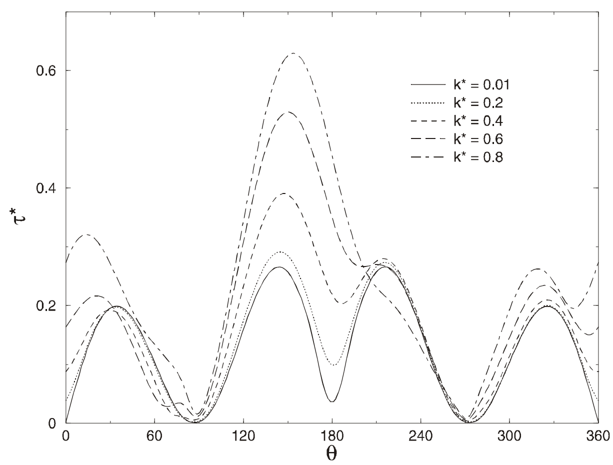

Figure 4: Shear stress of interacting inhomogeneities

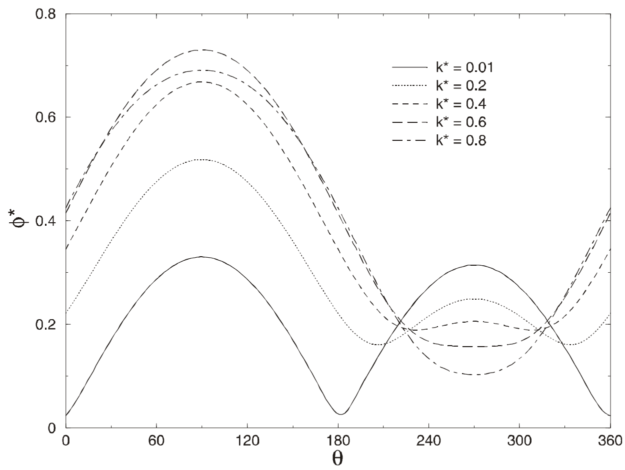

Figure 5: Potential of a single inhomogeneity

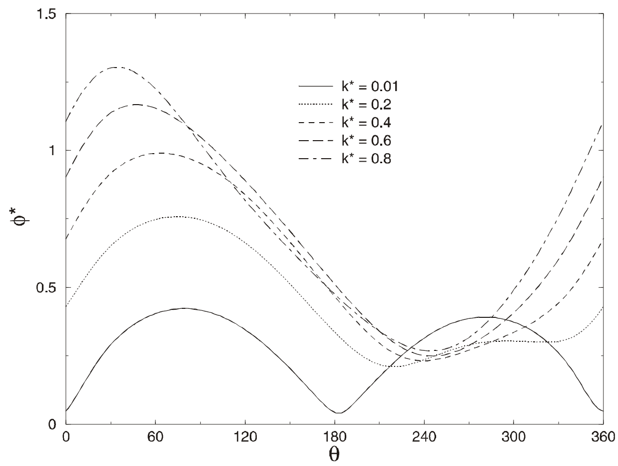

Figure 6: Potential of interacting inhomogeneities

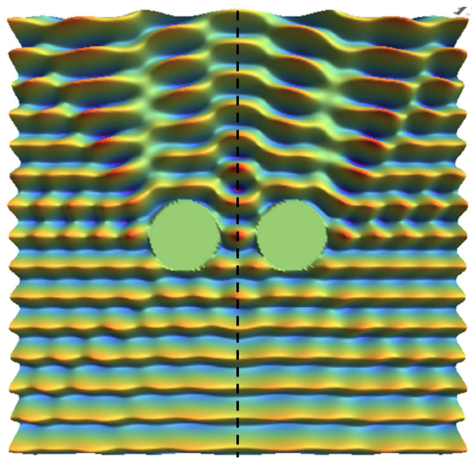

Figure 7: Wave field of two inhomogeneities

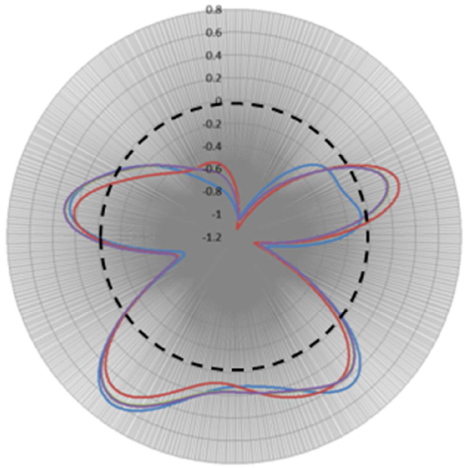

Figure 8: Displacement around the boundary

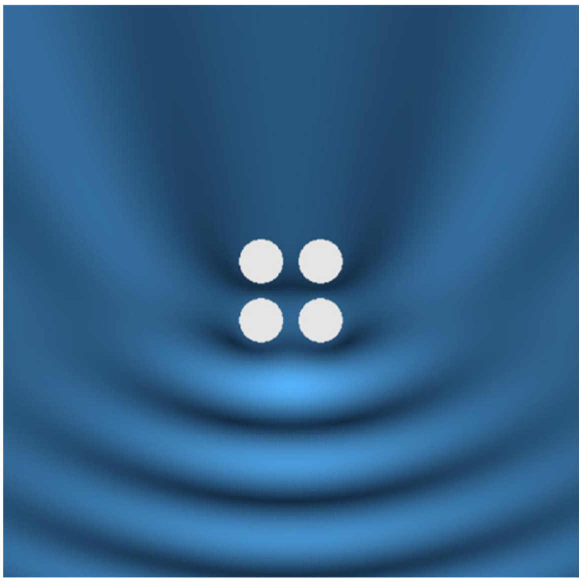

Figure 9: Displacement field due to four inhomogeneities

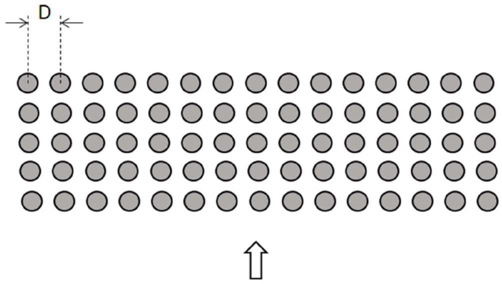

Figure 10: Array of multiple inhomogeneities

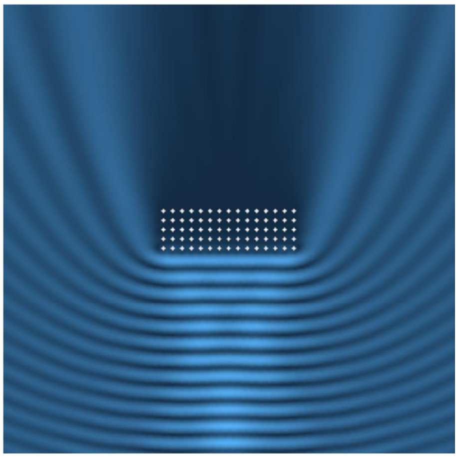

Figure 11: Displacement field for a normal incident wave, $k_M R=0.59$

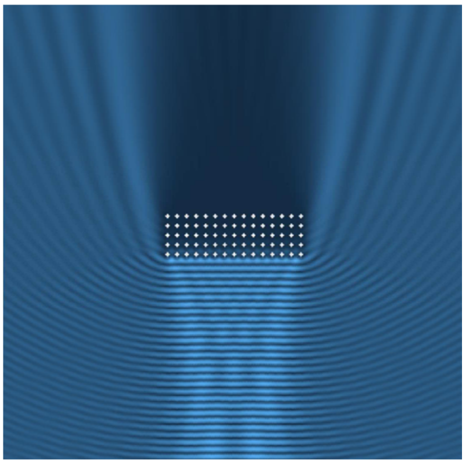

Figure 12: Displacement field for a normal incident wave, $k_M R=1.37$